Desalination and Water Treatment
www.deswater.com
doi: 10.1080/19443994.2014.940396

56 (2015) 266–273
September

Taylor & Francis
Taylor & Francis Group

Evaluation of the Cd removal efficacy from aqueous solutions using titania PVA-alginate beads

Ani Idris*, Zohreh Majidnia

Faculty of Chemical Engineering, Department of Bioprocess Engineering, Institute of Bioproduct Development, Universiti Teknologi Malaysia, 81310 Skudai, Johor, Malaysia, Tel. +60 19 7776054, +60 07 5535603; Fax: +60 07 5581463; email: ani@cheme.utm.my (A. Idris), Tel. +60 17 7530793; email: zmajidnia@yahoo.com (Z. Majidnia)

Received 12 February 2014; Accepted 2 June 2014

ABSTRACT

An investigation was conducted on photocatalytic reduction and physical adsorption of Cd (II) in titania PVA-alginate beads. In order to determine the kinetics of photocatalytic process, the influence of the initial concentration was examined in detail. An exact analysis on the percentage of the initial reduction rate versus time at different initial concentrations of Cd(II) showed that with an increase in the initial concentration, the rate of substrate conversion reduced. It was also revealed that the beads containing the TiO_2 nanoparticles can be easily isolated from the aqueous solutions after the sorption process and can be reused for at least six times before it loses its initial properties. The reduction of Cd(II) with titania PVA-alginate beads fitted the pseudo-second-order kinetic model with a correlation coefficient (R^2) of 0.9993.

Keywords: Photocatalyst; Titania beads; Titanium oxide; Langmuir–Hinshelwood model; Regeneration

1. Introduction

Pollution of heavy metals in water has received vast attention because of their toxic effects at low concentration. Some of these metals can be accumulated in tissues of human body and threaten the health [1,2]. Amongst all, cadmium is known as the most toxic heavy metal [3]. There are many conventional methods for removing these pollutants, including ion exchange, precipitation electrochemical, solvent extraction, and reverse osmosis that are mostly based on applications in single systems that consist of either metal ions or organic solutes [4]. It should be noted that the traditional separation techniques suffer from many disadvantages, for instance, producing sludge leading to high-disposal costs, possibly generating secondary toxic compounds, and high cost [5,6]. Due to the flexible design and operation offered by the adsorption process, adsorption has been known as one of the most efficient and popular methods for removing the above-mentioned pollutants from wastewaters [7,8].

Titanium dioxide is known to be the most effective heterogeneous photocatalyst to reduce and oxidize the organic and inorganic substrates in photocatalysis process [9–11]. Heterogeneous photocatalysis (HP) with TiO_2 and UV light is known as a growing technology that can be applied to remove or transform a number

*Corresponding author.

of pollutants through some reductive or oxidative mechanisms [12]. This process is capable of removing rapidly the toxic organics as well as microbiological pollutions. A review on the literature shows that photocatalytic transformation of metal ions that includes recovery of valuable metals has been less investigated compared with other techniques. In this sense, HP can be potentially applied to eliminate Cd(II) from aqueous solutions; although, this process has not received adequate attention [13].

Removal of cadmium was studied at pH 7 using TiO_2 Degussa as photocatalyst, and either formate or methanol as hole scavengers [14]. Their result revealed that in the absence of organic additives, approximately 60% of cadmium (concentration is 30 ppm) was removed from the solution by adsorption. Some researchers used thiourea-modified magnetic ion-imprinted chitosan/TiO_2 (MICT) for effective cadmium adsorption degradation. They found maximum adsorption capacity of cadmium was 256.41 mg/g [15]. In another study, the researchers investigated the use of thiolactic acid (TLA)-modified TiO_2 nanoparticles for removal of aqueous cadmium from simulated wastewaters. The results indicated approximately 90% of cadmium was removed by both adsorption and reduction processes onto the TLA-modified TiO_2 [9]. Visa et al. [16] presented the results of cadmium removal on fly ash (FA) with methyl orange-modified surface and its combinations with TiO_2. Adsorption efficiencies over 95% were registered on 25% TiO_2 mixtures with modified FA [16]. In another research, photocatalysis/hydrogen peroxide processes had been employed for the removal of cadmium. Results shown that the optimum efficiencies of Cd(II) removal was 97.7% at pH 11 [17].

In most of the above-mentioned studies, TiO_2 nanoparticles have been used either in a film or powder form. However, in the present study, an attempt was made to embed TiO_2 nanoparticles in PVA-alginate matrix in a bead form with the intention of prolonging its lifespan and further, remove the Cd(II) from the aqueous solution. The ability of the photocatalyst to be reused is an essential practical aspect of the cost effectiveness in every related process. Enhancing the TiO_2 reuse ability would result in a cheaper and environmentally friendly process.

2. Materials and methods

2.1. Materials

Acetylacetone, Titanium isopropoxide, urea, PVA, and alginate were purchased from Sigma–Aldrich. Cd(II) solution and ethanol were purchased from Merck.

2.2. Methods

2.2.1. TiO_2 powder synthesis

Two milliliter titanium isopropoxide and 2 ml acetylacetone were initially mixed and vigorously stirred and then added to 40 ml ethanol solution at room temperature. Then, this mixture and urea solution (0.5 g of urea added to 10 ml DI water) were added drop wise in to 40 ml DI water, stirring continuously at room temperature. The resultant mixture was pale yellow with a pH value of 5.6. This mixture was stirred vigorously for one hour. Then, the mixture was transferred into a 120 ml teflon-lined stainless steel autoclave that was heated at 150˚C for 18 h. The contents were cooled at room temperature. Then, the yellowish white sample was centrifuged with deionized water and ethanol. The sample was dried at 80˚C for 3 h and then stored in a clean dark-colored dry bottle for future use [18].

2.2.2. Titania PVA-alginate beads preparation

By mixing 1 g of alginate, 12 g of PVA, and 0.1 g of titanium oxide into distilled water, 100 mL precursor solution was made. Initially, 12 g of PVA was stirred in 72 mL of distilled water for about 5 h under conventional heating at 80˚C, but the alginate was stirred in 20 mL of distilled water in a different beaker. After conventional heating, PVA was put in a microwave to heat for another 4 min in order to ensure a complete dissolution. The alginate and PVA solutions were mixed in a beaker and then poured into the titanium oxide powder. The solution was continuously stirred to ensure homogeneity. The solution was then poured into a solution containing a mixture of 2% calcium chloride ($CaCl_2$) and 6% of boric acid solution by means of a peristaltic pump. The beads were allowed to remain in the $CaCl_2$ and boric acid solution for 24 h. After that they were washed with distilled water several times and stored in deionized water for future use [19].

2.2.3. Characterization of the TiO_2 nanoparticles

Morphological and structural analysis of the samples was done by a field emission scanning electron microscope (FESEM, Hitachi S4800) and a high resolution transmission electron microscope (HRTEM, JEOL-JSM-6360). Using an X-ray ($2\theta = 20$–90) diffractometer (XRD, Bruker D-8 Advance) that used

the Cu K_α radiation of wavelength $\lambda = 1.5406$ Å [18], the phase was identified. The Fourier Transform Infrared Spectroscopy (FTIR) measurements were conducted between 400 and 4,000 cm^{-1} [20]. By means of FTIR spectrum, major functional groups in the adsorbent can be quantitatively analyzed [21].

2.2.4. Photocatalytic activity under sunlight

The reactions were carried out under sunlight irradiation. Ten grams of titania PVA-alginate beads was placed in 200 ml of Cd(II) solution in a 500 ml beaker for 180 min. Every 15 min, 5 ml samples were taken out for Cd(II) analysis (Fig. 1). The Cd(II) initial concentration in the solutions was varied from 50, 100 to 200 mg/l. Additionally, the impact of pH on Cd(II) sorption was examined at different pH ranges, between 3.0 and 10.0. For the initial solution, the pH value was fixed to the required pH value through addition of HCl for acidic condition or NaOH for alkaline condition [22]. The effect of temperature was also studied by performing experiments at three different temperatures (25, 35, and 45°C).

2.2.5. Desorption experiments

Consecutive adsorption–desorption cycles were used to examine the TiO_2 bead reusability. By means of the same titania PVA-alginate beads, the adsorption experiments were iterated. Using desorbing agent (HCl 50 ml of 0.1 M) in 250 ml Erlenmeyer flasks, the metal-loaded titania PVA-alginate beads (10 g) were washed. During each desorption process, the flasks containing the beads in the HCl solution were placed on a shaker and this was rotated at 100 rpm for 60 min at room temperature, and an analysis was carried out on the supernatant for the desorbed metal ions. AAS was then employed to determine the concentration of Cd(II) that is desorbed in acidic solution. In order to investigate the regeneration behavior of the adsorbent, the before-used titania PVA-alginate beads were recycled and reused as the regenerated sorbent for five repeated sorption–desorption cycles [21,23].

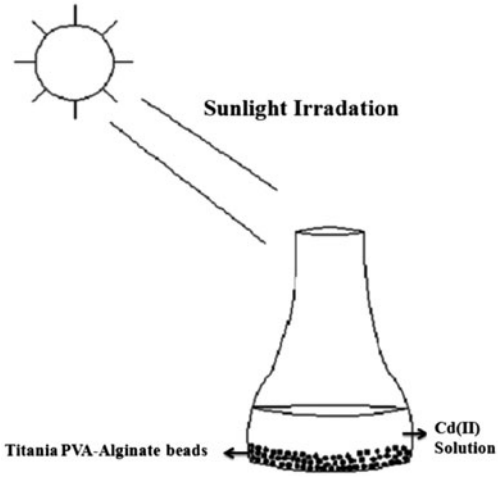

Fig. 1. Schematic diagram of photocatalytic activity under sunlight irradiation.

3. Results and discussion

3.1. Morphology of titanium oxide nanoparticles

Fig. 2 illustrates the XRD patterns of powders resulted from the hydrothermal treatment. As can be seen, the peaks of the powdered material were resulted from (1 0 1), (0 0 4), (2 0 0), (1 0 5), (2 1 3), (1 1 6), (2 1 5), and (3 0 3) reflections. It is easy to index the reflection peaks to anatase TiO_2 with lattice constants of $a = 3.784$ Å and $c = 9.512$ Å (JCPDS: No. 84–1286). It should be noted that in the XRD pattern, any characteristic peak that was relevant to other crystalline forms was not found.

Fig. 3 presents the FTIR spectra of TiO_2 powder. A broad band can be observed between 3,200 and 3,600 cm^{-1} on samples, which results from O–H stretching and deformation vibrations of weak-bound water. Between 400 and 800 cm^{-1}, there are bands that result from the vibrations of tin oxide [24], whereas the sharp bands in the range of 1,400–1,700 cm^{-1} are related to the CH_2– and $–CH_3$ band.

The low- and high-magnification FESEM images of the prepared powder samples are displayed in Fig. 4(a) and (b), respectively. The nanoparticles are uniformly distributed throughout the sample and the sizes of the particles are fairly small. The average size

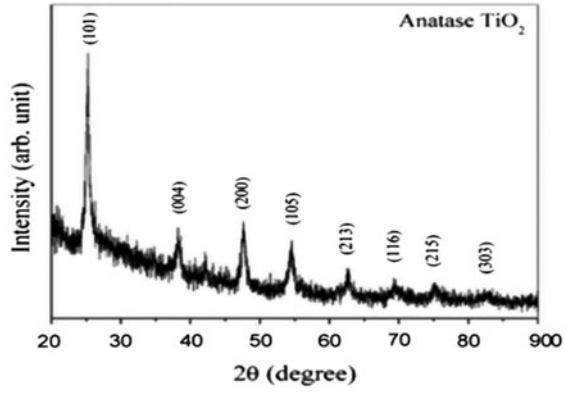

Fig. 2. XRD patterns of the as-prepared TiO_2 nanoparticles.

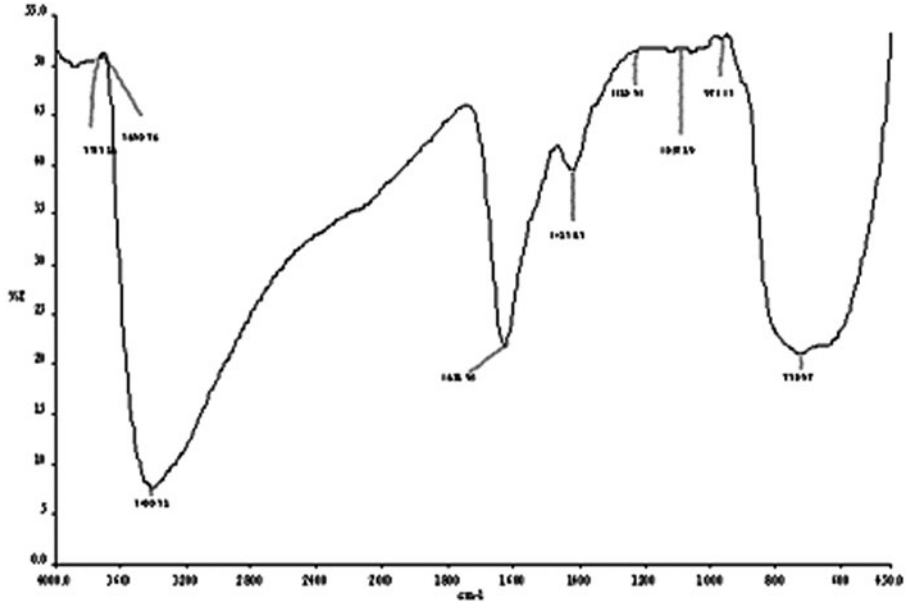

Fig. 3. FTIR analyses of titanium oxide nanoparticles.

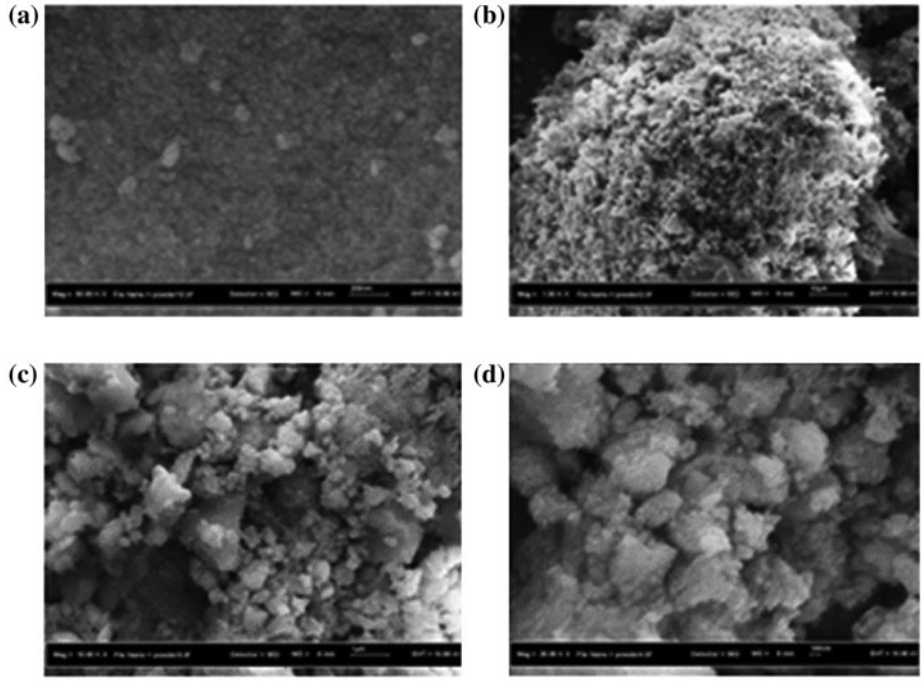

Fig. 4. (a) and (b) are the FESEM images and (c) and (d) are the TEM images for different magnification of TiO_2 nanoparticles.

was determined using HRTEM analysis. Typical low-and high-magnification HRTEM images of the sample are shown in Fig. 4(c) and (d), respectively, which also revealed the formation of uniform TiO_2 nanoparticles. The average particle size was approximately 15 nm as obtained from Fig. 4(d). The minimum and maximum particle sizes lie close to the average particle size.

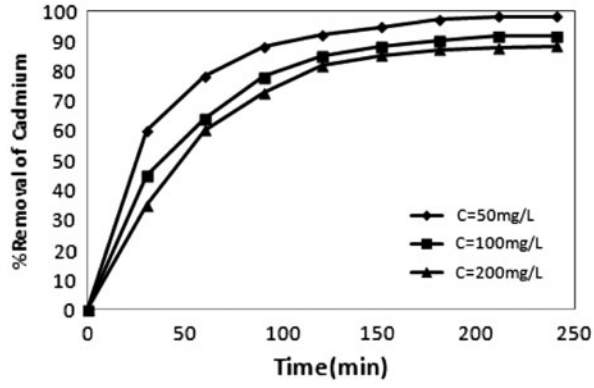

Fig. 5. The adsorption of Cd(II) ions with titania PVA-alginate beads at different concentration of Cd(II) at pH 7.

3.2. Effect of initial concentration solution on adsorption capacity

Fig. 5 shows the percentage of cadmium (II) reduction as a function of illumination time at pH 7 at various initial concentrations of Cd(II). Under all pH conditions, the uptake of Cd(II) ion with respect to contact time occurred in two stages. In the first hour of sorbent–sorbet contact, a rapid metal uptake happened, known as the first stage [23]. It was followed by the second stage; a slower metal uptake rate and an equilibrium spreading over a noticeably lower period. Such an adsorption pattern has been used in numerous studies in case of other metal ions or adsorbents. Initially, the rapid stage may be because of the high availability of active sites on the biosorbent. As shown by the slower phase, upon gradual occupancy of these sites, sorption occurs less efficiently.

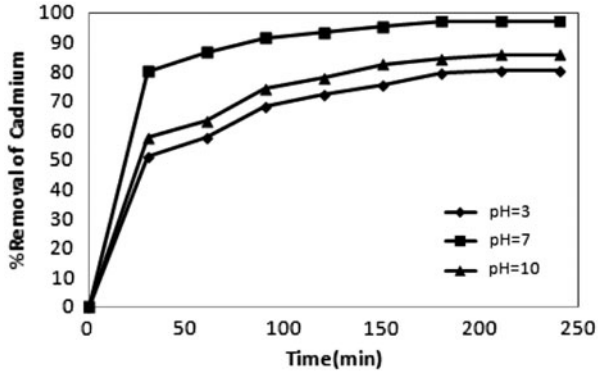

Fig. 6. The adsorption of Cd(II) ions with titania PVA-alginate beads at pH 3, 7, and 10 [experimental conditions: Cd(II) solution concentration = 50 mg/l].

3.3. The effect of pH on adsorption capacity

The Cd(II) removal at different pH is shown in Fig. 6. It can be seen that maximum Cd(II) removal occurred at pH 7, whereas Cd(II) removal rate improved along with the pH ranging from 3.0 to 7.0 and further increase in pH up to 10 did not show improvement in the Cd(II) removal efficiency. When the photocatalyst process was performed at pH 7, 100% of the cadmium was removed in 3 h compared with the other pH conditions which did not reach 100% cadmium removal even after 3 h of illumination time. Percentage of cadmium reduction at pH 3, only reached 70% within 3 h, whilst at pH 10, cadmium removed reached 75% within 3 h illumination time.

Increasing pH decreases the concentration of H^+, therefore, reducing the competition between metal ions and protons for adsorption sites on the particle surface. As pH increases there will be a decrease in positive surface charge resulting in lowering of electrostatic repulsion between the surface and metal ions, and thus, explained why pH 7 is an optimum pH condition for cadmium reduction [23].

3.4. The effect of temperature on adsorption capacity

Fig. 7 shows the effect of temperature on the batch adsorption of Cd(II). Higher removals for cadmium ions studied were observed in the lower temperature range. Furthermore, the maximum removals for (99%) Cd(II) were observed at 25°C. So, a decrease in uptake of heavy metal cations with the rise in temperature was observed. This was due to the increasing tendency of adsorbate ions to desorb from the interface to the solution with increasing temperature [25].

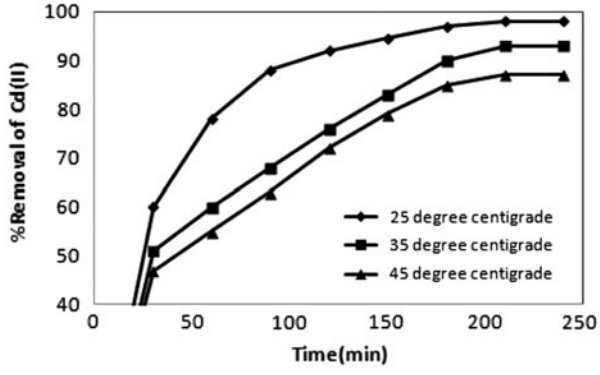

Fig. 7. The adsorption of Cd(II) ions with titania PVA-alginate beads at different temperatures (°C) [experimental conditions: Cd(II) solution concentration = 50 mg/l and pH 7].

3.5. Kinetic modeling

The kinetics of absorption of Cd(II) ions onto the adsorbent materials was described using two models; the Langmuir–Hinshelwood first-order [26] and the pseudo-second-order rate model.

A pseudo-second-order rate model as described [27] was used to describe the kinetics of absorption of Cd(II) ions onto the adsorbent materials. The differential equation for chemisorptions kinetic rate reaction is expressed in (Fig. 8):

$$q = (C_o - C_t)\frac{V}{m} \tag{1}$$

$$\frac{dq_t}{dt} = k(q_e - q_t)^2 \tag{2}$$

where k is the rate constant of pseudo-second-order equation (L/mg h).

For the boundary conditions $t = 0$ to $t = t$ and $q_t = 0$ to $q_t = q_t$, the integrated form of Eq. (2) becomes:

$$\frac{1}{q_e - q_t} = \frac{1}{q_e} + kt \tag{3}$$

Eq. (3) can be rearranged to obtain a linear form of equation as:

$$\frac{t}{q_t} = \frac{1}{kq_e 2} + \left(\frac{1}{q_e}\right)t \tag{4}$$

If the initial sorption rate h (mg/L h) is:

$$h = kq_e 2 \tag{5}$$

Then Eqs. (4) and (5) will become:

$$\frac{t}{q_t} = \frac{1}{h} + \frac{1}{q_e}t \tag{6}$$

The kinetic plots of t/q_t versus t for Cd(II) ions sorption are presented in Fig. 9. The relationships are found to be linear and the values of the correlation coefficient (R^2) suggest a strong relationship between the parameters. The correlation coefficient R^2 was found to have extremely high value of (>0.99) and the theoretical q_e values agree with the experimental ones. The results suggest that the pseudo-second-order sorption mechanism was predominant and the overall rate constant of each of the sorbent appeared to be controlled by the chemisorption process. Thus, the sorption process of each ion follows the pseudo-second-order kinetic model.

Table 1 shows the values of the constants obtained from Langmuir–Hinshelwood first-order and the pseudo-second-order rate equations for the different Cd(II) concentrations. The results illustrate that cadmium removal in aqueous solution fitted the pseudo-second-order rate equations better with higher R^2 value ($R^2 = 0.9993$) compared with the Langmuir–Hinshelwood first-order equations ($R^2 = 0.9383$).

3.6. Desorption and regeneration

Desorption and regeneration potential of titania PVA-alginate beads is an important factor since it determines the costs that are associated with the adsorption system. In the present research, at initial concentration of 50 mg/l, the Cd(II) desorption from the metal-loaded titania PVA-alginate beads occurred at pH 7. In case of the first cycle, Cd(II) desorption from the metal-loaded titania PVA-alginate beads led to 93.12% metal recovery. As Fig. 10 demonstrates the

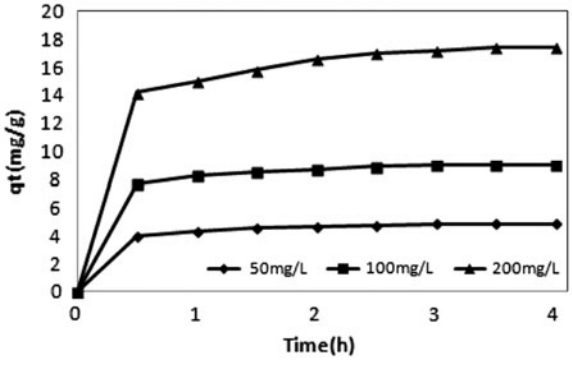

Fig. 8. The influence of initial concentration of Cadmium ions on the sorption kinetics of titania PVA-alginate beads.

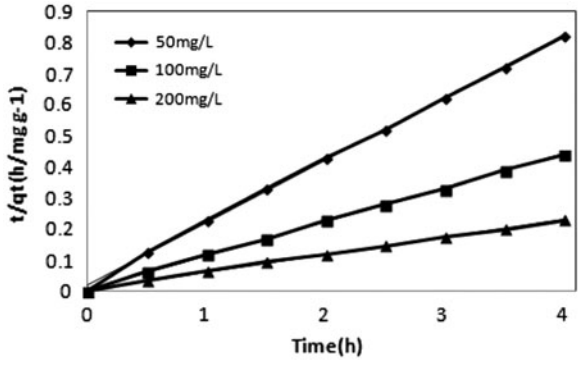

Fig. 9. Pseudo-second-order sorption kinetics of Cadmium ion onto titania PVA-alginate beads at various initial concentration.

Table 1
Pseudo-first-order and second-order apparent constant values for Cd(II) reduction

Initial Cd(II) concentration C_o (mg/L)	First order		Second order				
	Reaction rate, k_{app} (1/min)	R^2	r_o (mg/L min)	q_e (mg/g)	H (mg/g h)	K (g/mg h)	R^2
50	0.0191	0.9383	0.955	4.85	51.81	2.2	0.9989
100	0.0132	0.9029	1.32	9	136.9	1.7	0.9993
200	0.0117	0.9119	2.34	17.4	158.7	0.52	0.9992

percentage desorption for the metals does not reduce considerably during the five sorption–desorption cycles. The metal removing efficiency of Cd(II) on titania PVA-alginate beads was 93.12% during the first cycle and experienced a 4.9% reduction in desorption capability of titania PVA-alginate beads after the second cycle. From the third to the seventh cycle, only a small reduction in the sorption capability of titania PVA-alginate beads was observed. As a result, titania PVA-alginate beads can be recycled a minimum of six to seven times without notably losing their initial photacatalytic properties.

4. Conclusion

The present study showed that initial concentration of substrate has a considerable impact on the photoreduction of Cd(II). It was found that there will be a decrease in the percentage adsorption of Cd(II) if the initial Cd(II) concentration increases. This was expected since for a fixed adsorbent dosage, the total available adsorption sites were limited, hence leading to a reduction in percentage removal of the adsorbate corresponding to an increase in initial adsorbate concentration. Furthermore, it was found that the initial reaction rates were directly proportional to the catalyst concentration, which indicated the heterogeneous regime. However, it was observed that in excess of a critical concentration, the reaction rate decreased and become independent of the catalyst concentration. The photocatalytic reduction kinetics of Cd(II) on titania PVA-alginate beads was highly governed by the pseudo-second-order kinetics model. They showed that a surface reaction, where the Cd(II) was absorbed, was the controlling step of the process. Additionally, the results obtained from the recycled beads were very promising as it showed that the photocatalyst beads can be reused for at least six times.

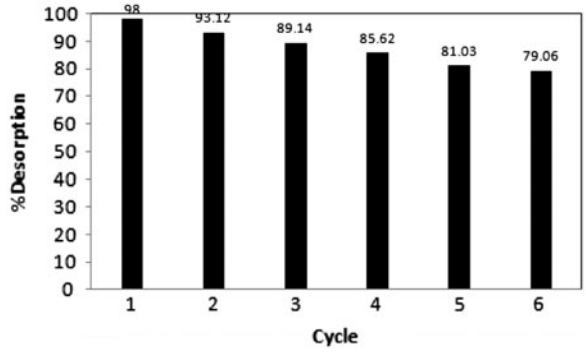

Fig. 10. The desorption capacity on recycling titania PVA-alginate beads.

List of symbols

DI — deionized water
λ — radiation of wavelength
r — photoreduction rate of the reactant (mg/L min)
c — concentration of the reactant (mg/L)
t — illumination time
k_r — reaction rate constant (mg/L min)
K_{LH} — adsorption coefficient of the reactant (L/mg)
K_{H_2o} — solvent adsorption constant
C_{H_2o} — concentration of the water
C_o — initial concentration of Cadmium (II) (mg/L)
k_{app} — pseudo-first-order rate constant
R^2 — correlation coefficient

References

[1] Q.X. Zhou, X.-N. Zhao, J.-P. Xiao, Preconcentration of nickel and cadmium by TiO_2 nanotubes as solid-phase extraction adsorbents coupled with flame atomic absorption spectrometry, Talanta 77 (2009) 1774–1777.
[2] R. Ertaş, N. Öztürk, Removal of lead from aqueous solutions by using chestnut shell as an adsorbent, Desalination Water Treat. 51 (2013) 2903–2908.
[3] G.-M. Zeng, X. Li, J.-H. Huang, C. Zhang, C.-F. Zhou, J. Niu, L.J. Shi, S.B. He, F. Li, Micellar-enhanced ultrafiltration of cadmium and methylene blue in synthetic wastewater using SDS, J. Hazard. Mater. 185 (2011) 1304–1310.
[4] X. Li, G.M. Zeng, J.H. Huang, D.M. Zhang, L.J. Shi, S.B. He, M. Ruan, Simultaneous removal of cadmium ions and phenol with MEUF using SDS and mixed surfactants, Desalination 276 (2011) 136–141.

[5] A.N. Módenes, F.R. Espinoza-Quiñones, D.E.G. Trigueros, F.L. Lavarda, A. Colombo, N.D. Mora, Kinetic and equilibrium adsorption of Cu(II) and Cd(II) ions on *Eichhornia crassipes* in single and binary systems, Chem. Eng. J. 168 (2011) 44–51.
[6] A.B. Albadarin, C. Mangwandi, A.a.H. Al-Muhtaseb, G.M. Walker, S.J. Allen, M.N.M. Ahmad, Kinetic and thermodynamics of chromium ions adsorption onto low-cost dolomite adsorbent, Chem. Eng. J. 179 (2012) 193–202.
[7] A. Chen, G. Zeng, G. Chen, X. Hu, M. Yan, S. Guan, C. Shang, L. Lu, Zh. Zou, G. Xie, Novel thiourea-modified magnetic ion-imprinted chitosan/TiO_2 composite for simultaneous removal of cadmium and 2,4-dichlorophenol, Chem. Eng. J. 191 (2012) 85–94.
[8] Y. Pang, G. Zeng, L. Tang, Y. Zhang, Y. Liu, X. Lei, Zh Li, J. Zhang, G. Xie, PEI-grafted magnetic porous powder for highly effective adsorption of heavy metal ions, Desalination 281 (2011) 278–284.
[9] L.R. Skubal, N.K. Meshkov, T. Rajh, M. Thurnauer, Cadmium removal from water using thiolactic acid-modified titanium dioxide nanoparticles, J. Photochem. Photobiol., A 148 (2002) 393–397.
[10] A. Idris, E. Misran, N. Hassan, A.A. Jalil, C.E. Seng, Modified PVA-alginate encapsulated photocatalyst ferro photo gels for Cr(VI) reduction, J. Hazard. Mater. 227–228 (2012) 309–316.
[11] M. Kidwai, S. Bhardwaj, A.A. Jain, A green oxidation protocol for the conversion of secondary alcohols into ketones using heterogeneous nanocrystalline titanium (IV) oxide in polyethylene glycol, Green Chem. Lett. Rev. 5 (2012) 195–202.
[12] M.I. Litter, Heterogeneous photocatalysis: Transition metal ions in photocatalytic systems, Appl. Catal., B 23 (1999) 89–114.
[13] L. Murruni, G. Leyva, M.I. Litter, Photocatalytic removal of Pb(II) over TiO_2 and Pt–TiO_2 powders, Catal. Today 129 (2007) 127–135.
[14] V.N.H. Nguyen, R. Amal, D. Beydoun, Effect of formate and methanol on photoreduction/removal of toxic cadmium ions using TiO_2 semiconductor as photocatalyst, Chem. Eng. Sci. 58 (2003) 4429–4439.
[15] A. Chen, G. Zeng, G. Chen, X. Hu, M. Yan, S. Guan, C. Shang, L. Lu, Z. Zou, G. Xie, Novel thiourea-modified magnetic ion-imprinted chitosan/TiO_2 composite for simultaneous removal of cadmium and 2,4-dichlorophenol, Chem. Eng. J. 191 (2012) 85–94.
[16] M. Visa, R. Adrian Carcel, L. Andronic, A. Duta, Advanced treatment of wastewater with methyl orange and heavy metalson TiO_2, fly ash and their mixtures, Catal. Today 144 (2009) 137–142.
[17] M. Stylidi, D.I. Kondarides, X.E. Verykios, Visible light-induced photocatalytic degradation of acid orange 7 in aqueous TiO_2 suspensions, Appl. Catal., B 47 (2004) 189–201.
[18] R. Thapa, S. Maiti, T.H. Rana, U.N. Maiti, Anatase TiO_2 nanoparticles synthesis via simple hydrothermal route: Degradation of orange II, methyl orange and rhodamine B, J. Mol. Catal. A: Chem. 363–364 (2012) 223–229.
[19] A. Idris, E. Misran, N.M. Yusof, Photocatalytic reduction of Cr(VI) by PVA-alginate encapsulated γ-Fe_2O_3 magnetic beads using different types of illumination lamp and light, J. Ind. Eng. Chem. 18 (2012) 2151–2156.
[20] A.K. Yewale, F.C. Raghuwanshi, N.G. Belsare, R.V.J. Waghmare, T.S. Wasnik, K.B. Raulkar, A.S. Wadatkar, G.T. Lamdhade, Gas sensitivity of TiO_2 based thick film sensor to NH_3 gas at room temperature, Int. J. Adv. Eng. Technol. 2 (2011) 226–230.
[21] M. Iqbal, A. Saeed, S.I. Zafar, FTIR spectrophotometry, kinetics and adsorption isotherms modeling, ion exchange, and EDX analysis for understanding the mechanism of Cd^{+2} and Pb^{+2} removal by mango peel waste, J. Hazard. Mater. 164 (2009) 161–171.
[22] A. Idris, N. Hassan, R. Rashid, A.F. Ngomsik, Kinetic and regeneration studies of photocatalytic magnetic separable beads for chromium (VI) reduction under sunlight, J. Hazard. Mater. 186 (2011) 629–635.
[23] A. Idris, N.S.M. Ismail, N. Hassan, E. Misran, A.-F. Ngomsik, Synthesis of magnetic alginate beads based on maghemite nanoparticles for Pb(II) removal in aqueous solution, J. Ind. Eng. Chem. 18 (2012) 1582–1589.
[24] F. Sala, F. Trifirò, Oxidation catalysts based on tin-antimony oxides, J. Catal. 34 (1974) 68–78.
[25] G. Bereket, A. Zehra Aroguz, M.Z. Ozel, Removal of Pb(II), Cd(II), Cu(II), and Zn(II) from aqueous solutions by adsorption on bentonite, J. Colloid Interface Sci. 187 (1997) 338–343.
[26] V.K. Gupta, A. Rastogi, Equilibrium and kinetic modelling of cadmium(II) biosorption by nonliving algal biomass Oedogonium sp. from aqueous phase, J. Hazard. Mater. 153 (2008) 759–766.
[27] Y.S. Ho, G. McKay, The sorption of lead (II) ions on peat, Water Res. 33 (1999) 585–587.